



FINITE VOLUME NUMERICAL SIMULATION OF THREE-DIMENSIONAL NATURAL CONVECTION IN A GOLD-WATER NANOFUID INCLINED PRISMATIC SOLAR DIRECT ABSORBER ENCLOSURE WITH THE TIWARI-DAS VOLUME FRACTION MODEL

S. Kuharat*, O. Anwar Bég, Ali Kadir, Henry Leonard and Walid S. Jouri

Department of Mechanical and Aeronautical Engineering, Newton Building, Salford University, Manchester, M54WT, UK.

Emails: S.Kuharat@edu.salford.ac.uk (*Presenter), O.A.Beg@salford.ac.uk; A.Kadir@salford.ac.uk; h.leonard@salford.ac.uk; w.s.jouri@salford.ac.uk

1. INTRODUCTION

Nanofluids are increasingly being deployed in numerous energy applications owing to their impressive thermal enhancement properties. Motivated by these developments in the current study we present finite volume numerical simulations of natural convection in an inclined three-dimensional (3D) prismatic direct absorber solar collector (DASC) containing gold-water nanofluid. Steady-state, incompressible laminar Newtonian viscous flow is assumed. The enclosure has one hot (solar receiving) and one colder wall while all the remaining walls are adiabatic. ANSYS FLUENT computational fluid dynamics software is employed. The Tiwari-Das volume fraction nanofluid model is utilized to simulate nanoscale effects and allows a systematic exploration of volume fraction effects. The effects of thermal buoyancy (Rayleigh number), geometrical aspect ratio and enclosure tilt angle on isotherm and temperature contour distributions are presented with extensive visualization in both two and three dimensions. Grid-independence tests are included. Validation with published studies from the literature is also conducted. A significant modification in vortex structure and temperature distribution is computed with volume fraction, Rayleigh number, aspect ratio and tilt angle. Gold nano-particles even at relatively low volume fractions are observed to achieve substantial improvement in heat transfer characteristics.

MATHEMATICAL MODEL

The 3D models of heat transfer in the solar nanofluid absorber are designed in ANSYS FLUENT [1]. The geometric configuration is illustrated in Fig. 1. The fundamental equations for steady viscous, incompressible laminar flow and thermal convection are the three-dimensional time-independent Navier-Stokes equations and energy equation, which in a Cartesian coordinate system, take the following form:

D'Alembert mass conservation (3-D continuity)

$$\left[\frac{\partial u}{\partial x} + \frac{\partial v}{\partial y} + \frac{\partial w}{\partial z} \right] = 0 \quad (1)$$

x-direction momentum conservation

$$\rho \left[u \frac{\partial u}{\partial x} + v \frac{\partial u}{\partial y} + w \frac{\partial u}{\partial z} \right] = \rho F_x - \frac{\partial p}{\partial x} + \mu \left[\frac{\partial^2 u}{\partial x^2} + \frac{\partial^2 u}{\partial y^2} + \frac{\partial^2 u}{\partial z^2} \right] \quad (2)$$

y-direction momentum conservation

$$\rho \left[u \frac{\partial v}{\partial x} + v \frac{\partial v}{\partial y} + w \frac{\partial v}{\partial z} \right] = \rho F_y - \frac{\partial p}{\partial y} + \mu \left[\frac{\partial^2 v}{\partial x^2} + \frac{\partial^2 v}{\partial y^2} + \frac{\partial^2 v}{\partial z^2} \right] + F_{buoyancy} \quad (3)$$

z-direction momentum conservation

$$\rho \left[u \frac{\partial w}{\partial x} + v \frac{\partial w}{\partial y} + w \frac{\partial w}{\partial z} \right] = \rho F_z - \frac{\partial p}{\partial z} + \mu \left[\frac{\partial^2 w}{\partial x^2} + \frac{\partial^2 w}{\partial y^2} + \frac{\partial^2 w}{\partial z^2} \right] \quad (4)$$

Energy Equation

$$u \frac{\partial T}{\partial x} + v \frac{\partial T}{\partial y} + w \frac{\partial T}{\partial z} = \alpha m \left[\frac{\partial^2 T}{\partial x^2} + \frac{\partial^2 T}{\partial y^2} + \frac{\partial^2 T}{\partial z^2} \right] \quad (5)$$

Tiwari-Das model allows different concentrations (volume fraction) and types of metallic nano-particles. Where nanofluids properties can be calculate from follow equation:

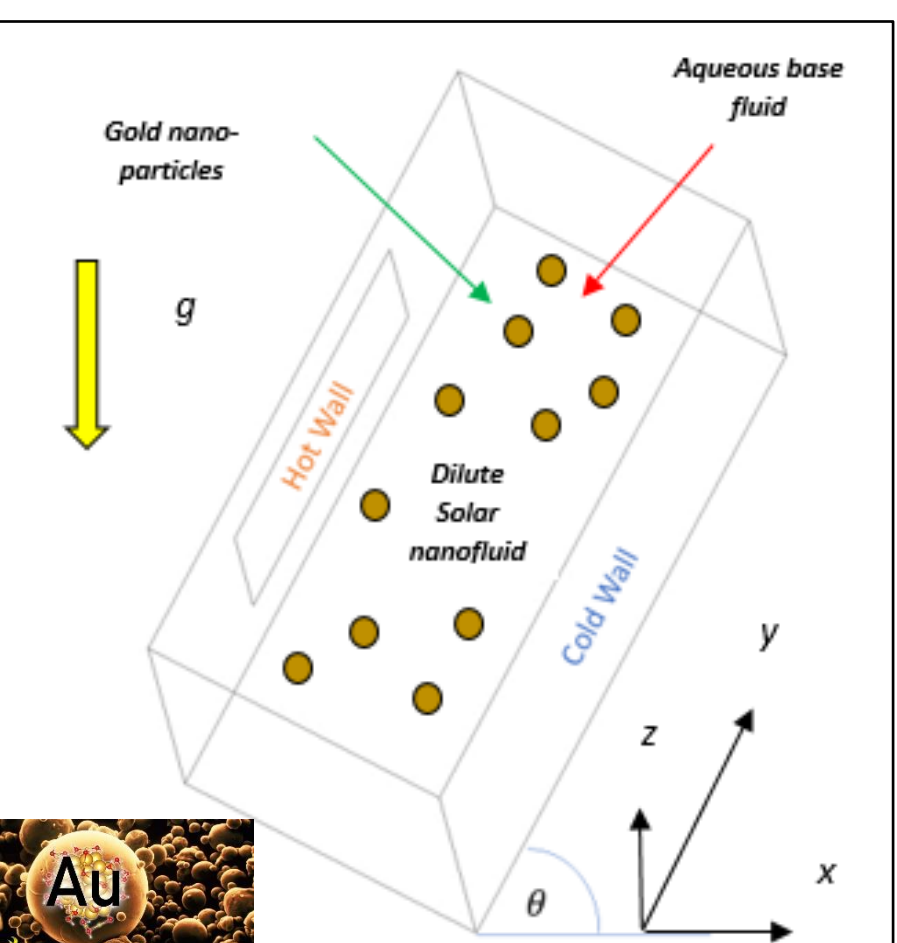
$$\phi = \frac{V_{np}}{V_f}, \mu_{nf} = \frac{\mu_f}{(1-\phi)^{2.5}}, \rho_{nf} = (1-\phi)\rho_f + \phi\rho_s,$$

$$C_{p,nf} = \frac{(1-\phi)(\rho C_p)_f + \phi(\rho C_p)_s}{\rho_{nf}}, k_{nf} = \frac{k_s + 2kf - 2\phi(k_f - k_s)}{k_s + 2kf - \phi(k_f - k_s)}$$

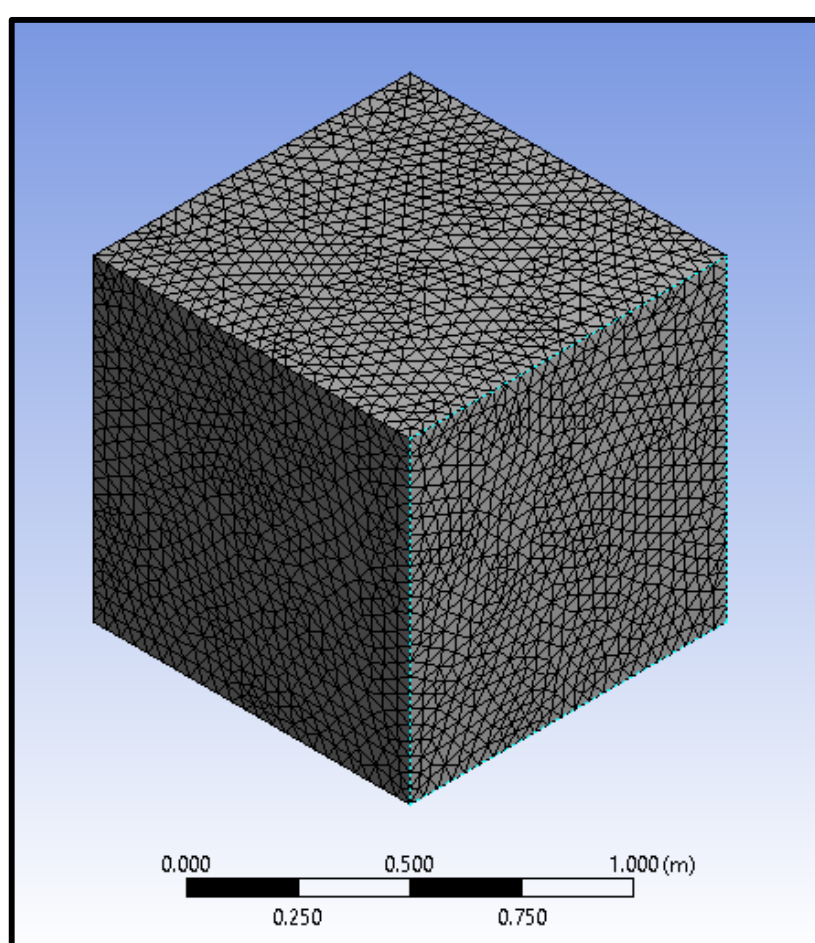
The key dimensionless parameters which computed are local Rayleigh number (Ra) and the average Nusselt number on the hot wall (\bar{Nu}).

$$\text{Rayleigh number: } Ra_y = \frac{g\beta}{\nu\alpha m} (T_s - T_\infty) y^3 \quad (12)$$

$$\text{Average Nusselt number: } \bar{Nu} = \frac{\bar{h}L}{k} = \frac{q_w C_{FD}(L)}{k(T_w - T_b)} \quad (13)$$



Figs. 1



Figs. 2

3. GRID STUDY & VALIDATION

An extensive mesh testing procedure was conducted to guarantee a grid-independent solution. The grid independence test has been performed on a cubical enclosure (i.e. aspect ratio =1) with $Ra = 10^5$, ϕ (volume fraction) = 0.02 i.e. 2% gold nano-particles by volume. The results of the mesh variation are shown in Fig. 3. It is evident that the simulations attain mesh-independent convergence with approximately 40,000 tetrahedral elements (Fig. 2). From Fig. 4 shows that the non-dimensional temperature along the horizontal centreline in the $Y/L=0.5$, confirms that the present results are close to the benchmark results. Furthermore, it also confirm that the grid resolution of the simulation is fine enough to obtain the independent results.

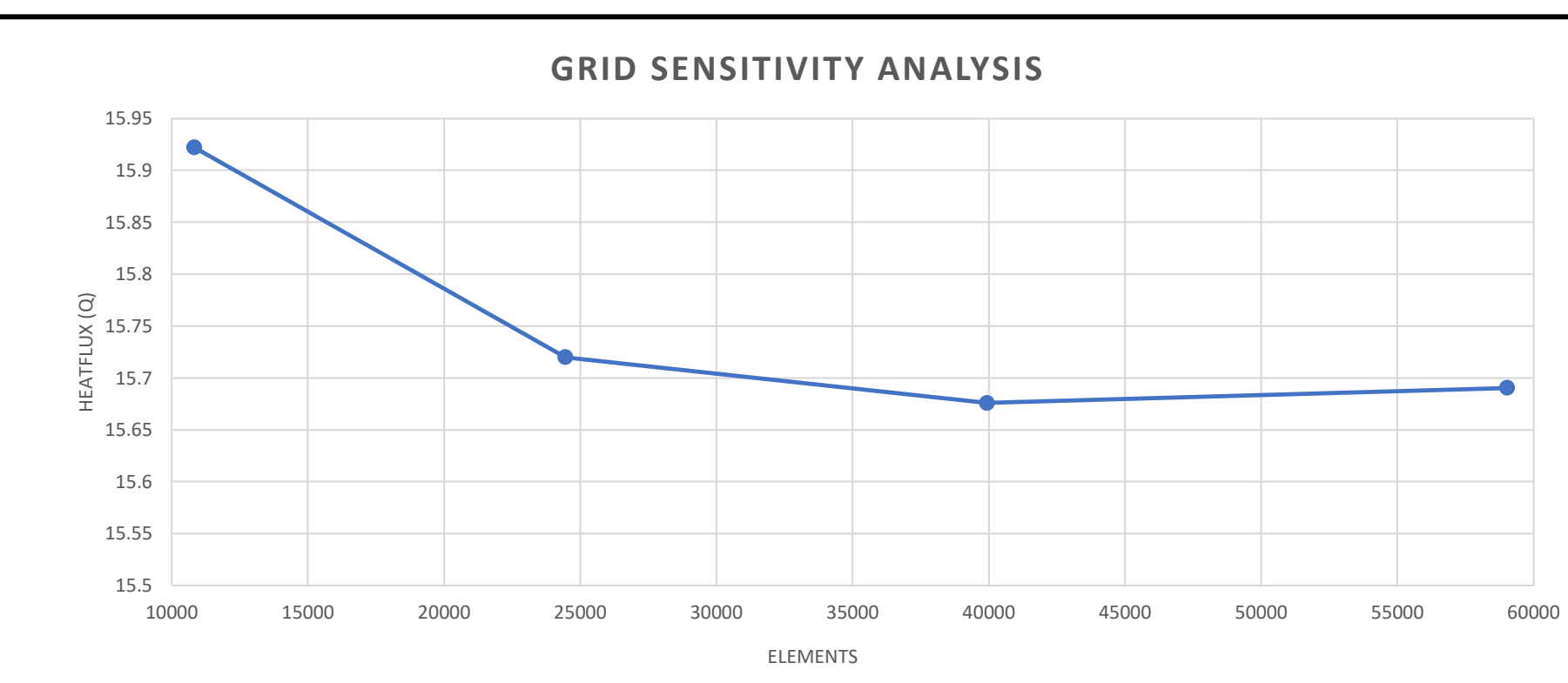


Fig. 3: Finite volume ANSYS FLUENT grid independence study

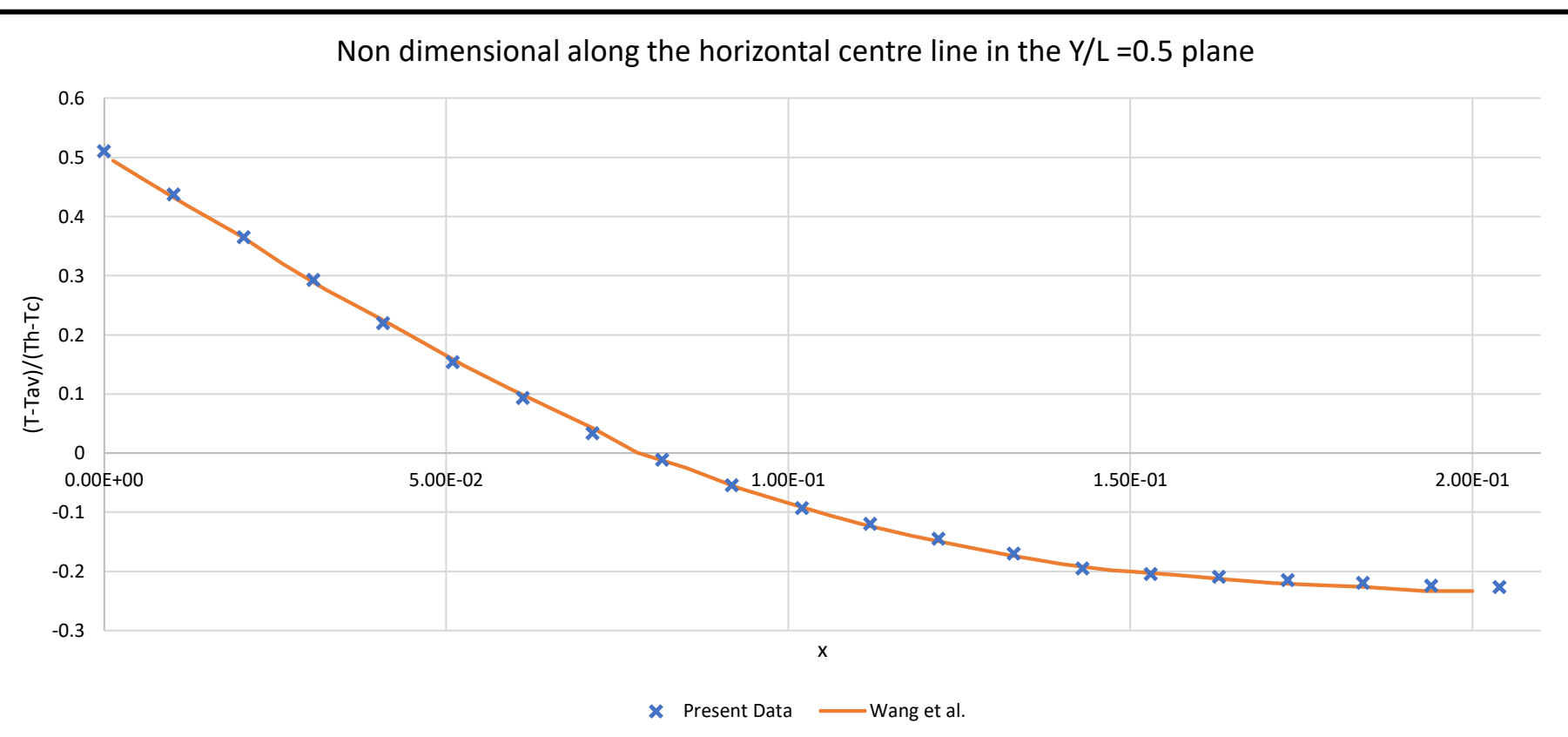


Fig.4 The non-dimensional temperature along the horizontal centreline in the Y/L=0.5

4. RESULTS AND DISCUSSION

INCLINATION EFFECT

Fig. 5 show the evolution in left hot wall 3-dimensional temperature contour plots with a progressive increase in tilt angle ($\alpha = 0, 10, 30, 45$ and 60 degrees) at Rayleigh number of $Ra = 10^5$. As the enclosure tilt angle is increased this the hotter zone expands steadily to occupy a greater area in the enclosure. The warm green contours are progressively replaced with hotter yellow contours and the colder blue zone is systematically compressed although it is not eliminated. The red hotter linear zone along the left edge is slightly expanded but does not grow to the full extent of the edge length. The stronger thermal buoyancy present contributes to enhancement in thermal diffusion and also enhances thermal boundary layer thickness at the left wall. This effect has also been computed by Ostrach [2] for Newtonian fluids. Scaling thermal buoyancy contribution via tilting the enclosure is therefore a simple but powerful mechanism for regulating temperature distribution in the solar collector.

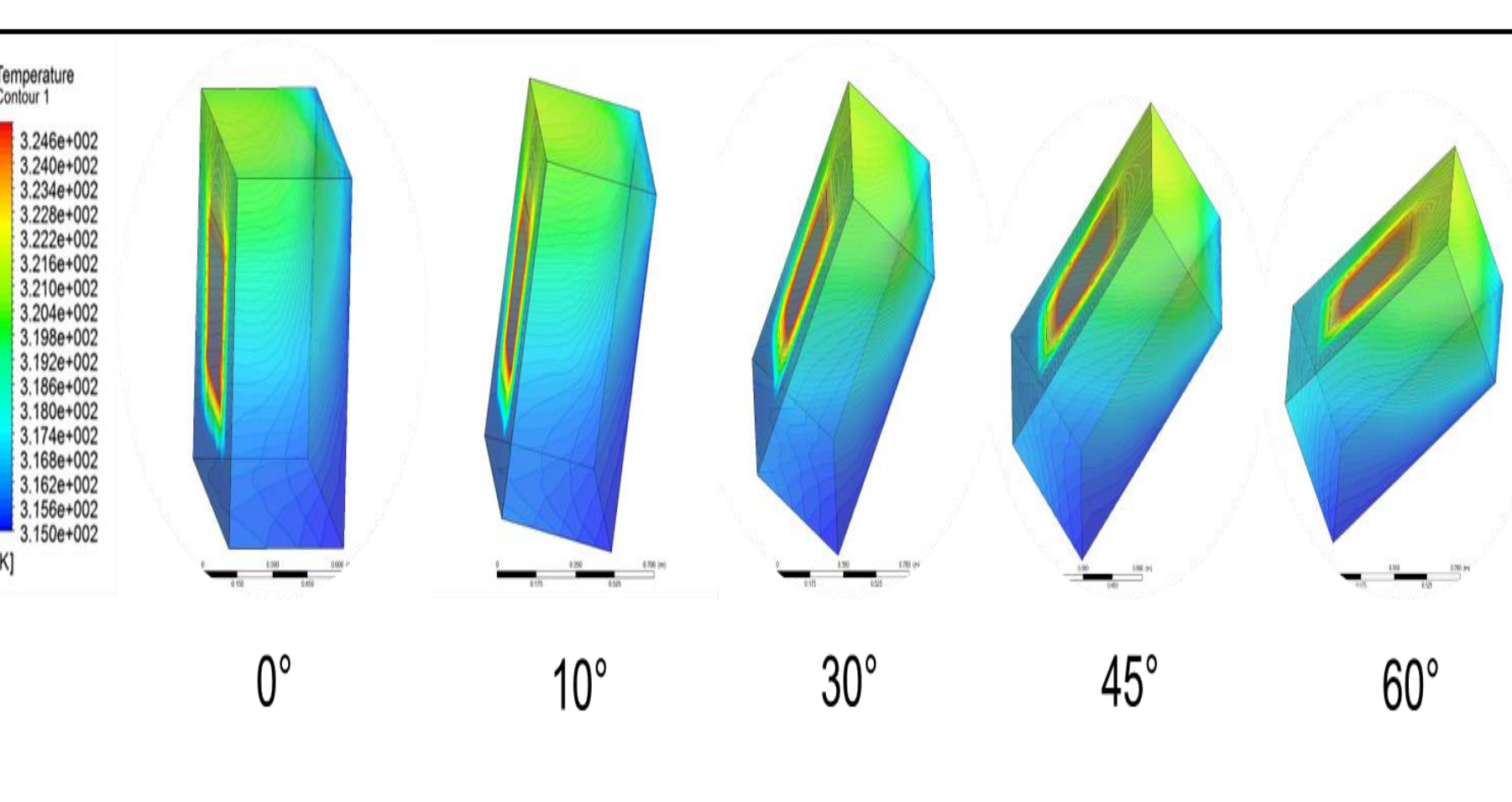


Fig. 5 Temperature Contour of Tilted Effect

VOLUME FRACTION EFFECT

Fig. 6 shows that heat flux is dramatically increased with greater nano-particle volume fraction. The presence of nano-particles mobilizes micro-convection and encourages thermal diffusion away from the wall. This achieves the thermal enhancement. Similar findings have been reported by numerous authors including Tafarroj et al. [3], Fattahi et al. [4] Balakin et al. [5] and Nasrin et al. [6] for both carbon-based and metallic nano-particles although they did not examine the case of gold.

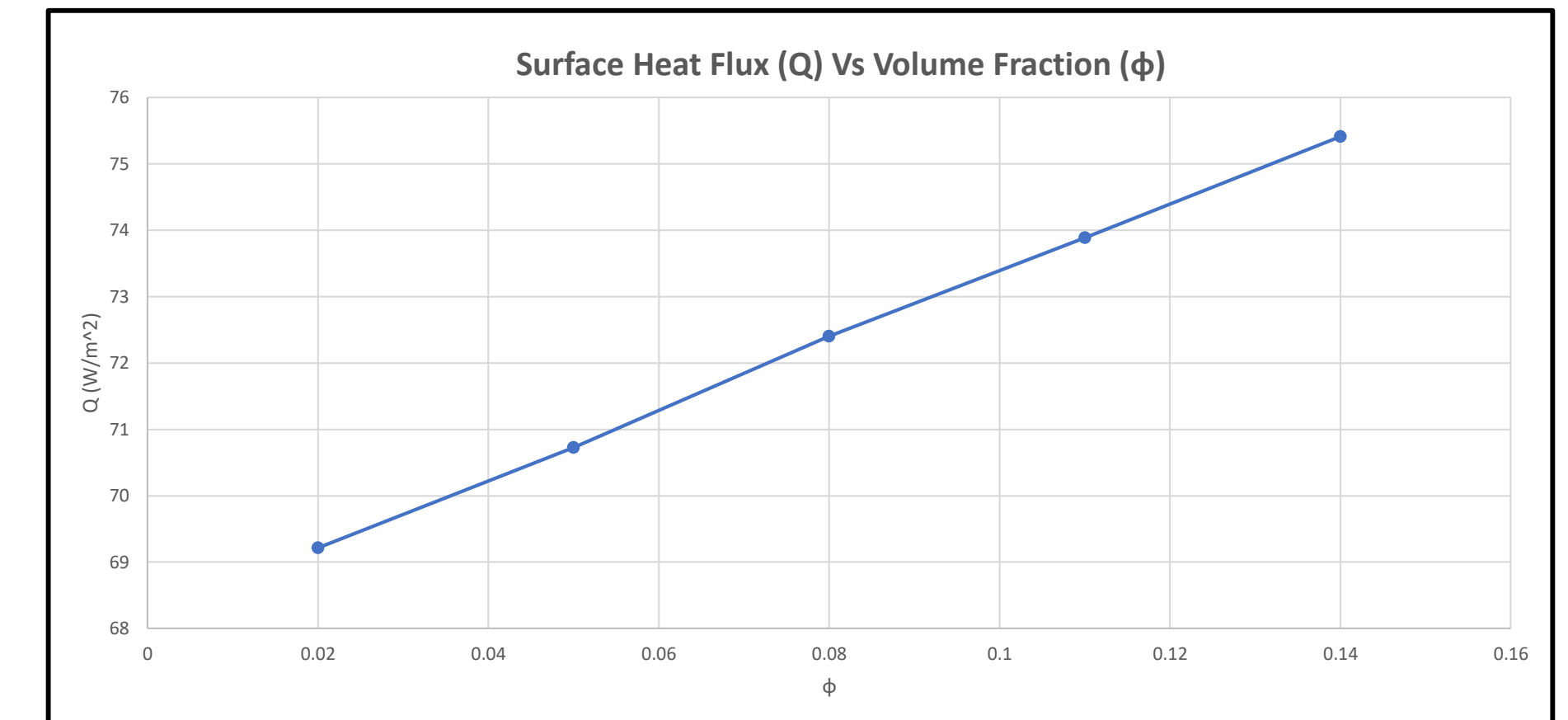


Fig. 6 Surface Heat Flux (Q) Vs Volume Fraction (phi)

ASPECT RATIO EFFECT

Figs. 7 depict the impact of geometric aspect ratio on 3-dimensional temperature contour plots where Rayleigh number is 100 times that in Figs 5 and 6. It is evident that again there is a marked expansion of the warmer yellow/green upper left zone deeper into the body of the enclosure with a gradual replacement of darker colder blue contours with lighter blue warmer ones further and further towards the base and the right wall. For the highest aspect ratio yellow/green contours reach the right cold wall although they are confined to the upper area only. This has also been computed by Esfandiary et al. [7] and Motlagh et al. [8] who also observed the deeper penetration of heat in enclosures with higher aspect ratio.

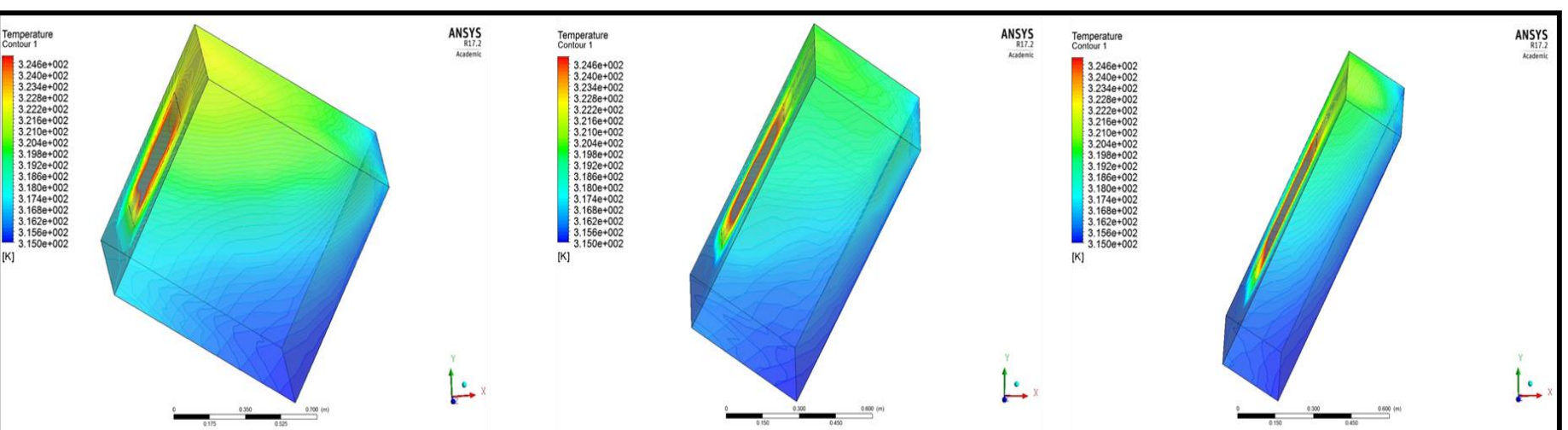


Fig. 7: Aspect ratio 3-dimensional temperature contour plots

Fig. 8 shows the influence of the Rayleigh number on full body 3-dimensional temperature contour plots. Initially there is an intensification in temperature contours only at the left hot wall with cooler light blue zones throughout the body of the enclosure and a cold blue zone at the far wall. This is modified to a localization of heat in the upper left zone of the enclosure with an increase in Rayleigh number from 10^3 to 10^4 . This trend continues to prevail with further increment in Rayleigh number up to 10^6 . However, at very high Rayleigh number of 10^7 the temperature distribution achieved is much more homogenous. Significantly more balanced thermal diffusion through the enclosure is therefore achieved with very strong thermal buoyancy effect and there is a contraction in the yellow/red hot zone on the hot wall for this scenario.

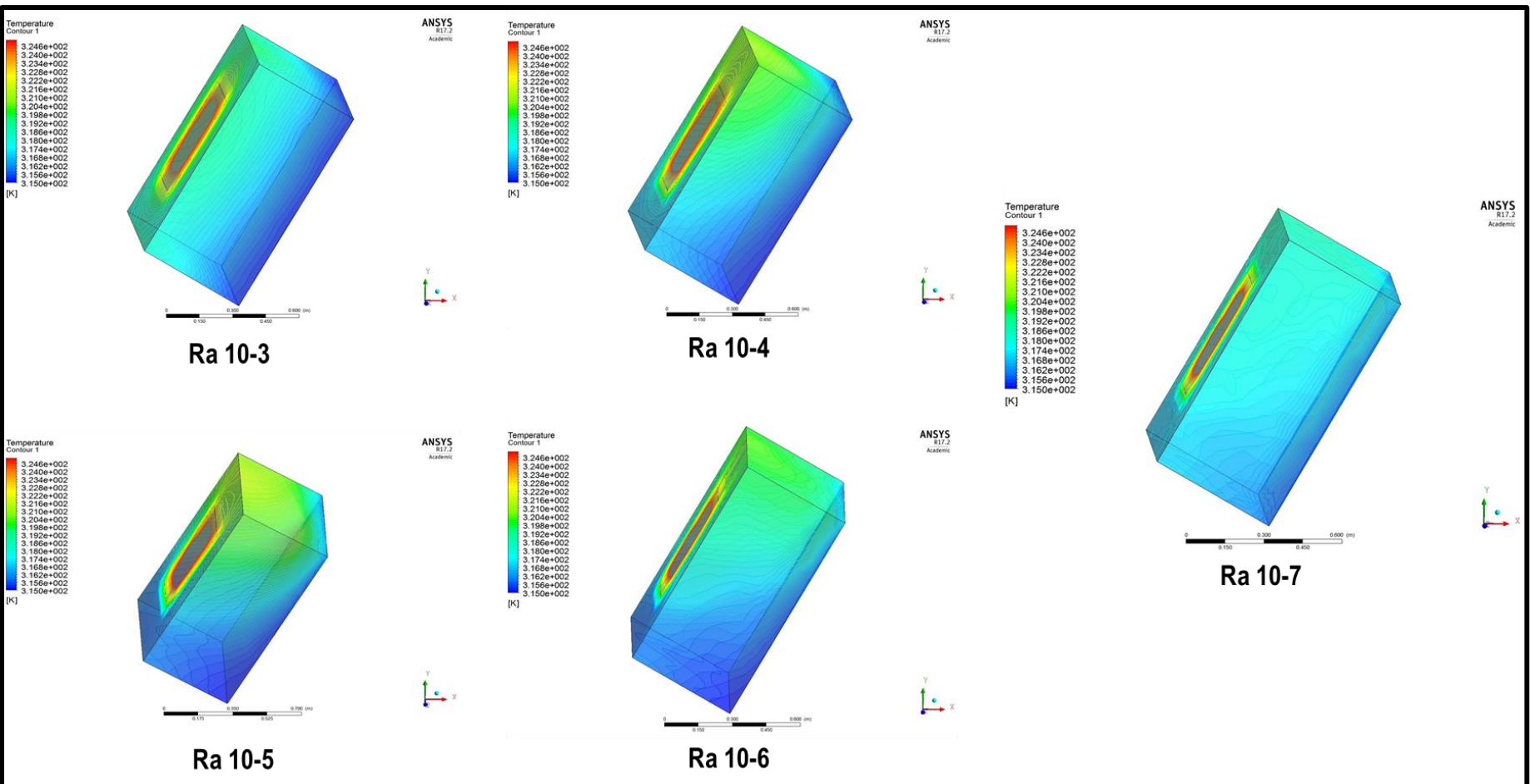


Fig. 8 : Rayleigh number 3-dimensional temperature contour plots.

5. CONCLUSIONS

- Higher aspect ratio leads to improved heat transfer in the regime with deeper penetration of warmer zones in the enclosure.
- Increasing Rayleigh number (thermal buoyancy force relative to viscous hydrodynamic force), induces an intensification in heat transfer from the left wall through the enclosure space and much more homogenous temperature distributions are eventually obtained.
- With increasing nano-particle volume fraction, heat penetrates more effectively into the enclosure from the hot wall and temperature magnitudes are enhanced.
- With greater inclination of the enclosure there is a progressive elevation in heat transfer from the left hot face (heated wall) towards the opposite cold wall, and temperatures are elevated mainly in the upper left zone with a more extensive warming in the central zone.
- Heat flux is dramatically increased with greater nano-particle volume fraction, and aspect ratio whereas it is suppressed with greater inclination of the enclosure.
- ANSYS FLUENT is a powerful tool for nanofluid solar collector simulation and is presently being explored for other configurations, non-Newtonian nano-liquids in addition to experimental rig designs.

REFERENCES

- [1] Sireetorn Kuharat and O. Anwar Bég, Simulation of a nanofluid-based annular solar collector, *ICHTFM 2018: 20th International Conference on Heat Transfer and Fluid Mechanics, Istanbul, Turkey, August 16 – 17 (2018)*.
- [2] S. Ostrach, Natural convection in enclosures, *Advances in Heat Transfer*, 8, 161-227 (1972).
- [3] M.M. Tafarroj et al., CFD modeling and predicting the performance of direct absorption of nanofluids in trough collector, *Applied Thermal Engineering*, 148, 256-269 (2019).
- [4] E. Fattahi et al., Lattice Boltzmann simulation of natural convection heat transfer in nanofluids, *International Journal of Thermal Sciences*, 52, 137-144 (2012).
- [5] B. Balakin et al., Direct absorption solar collector with magnetic nanofluid: CFD model and parametric analysis, *Renewable Energy*, 136, 23-32 (2019).
- [6] R. Nasrin et al., Effect of Prandtl number on free convection in a solar collector filled with nanofluid, *Proc. Eng.*, 56, 54-62 (2013).
- [7] M. Esfandiary et al., Natural convection of Al2O3-water nanofluid in an inclined enclosure with the effects of slip velocity mechanisms: Brownian motion and thermophoresis phenomenon, *International Journal of Thermal Sciences*, 105, 137-158 (2016).
- [8] S. Y. Motlagh et al., Natural convection of Al2O3-water nanofluid in an inclined cavity using Buongiorno's two-phase model, *International Journal of Thermal Sciences*, 111, 310-320 (2017).